# Homogeneous versus heterogeneous zeolite nucleation : a SAXS-WAXS study

# Homogeneous Versus Heterogeneous Zeolite Nucleation. A SAXS-WAXS Study

**Theo P.M. Beelen, Wim H. Dokter, Harold F. van Garderen and Rutger A. van Santen**

**Schuit Institute of Catalysis**
**Eindhoven University of Technology**
**P.O. Box 513, 5600 MB EINDHOVEN, The Netherlands**

Transformations of zeolite precursors have been followed during the induction or aging period preceding crystallization using small angle scattering with x-rays (SAXS) on the in situ preparation of silicalite. To study dynamics of the transformations high-brilliance synchrotron radiation was applied. To observe the onset of crystallization accurately and to distinguish the growth of crystalline and , in the same experiment also in situ wide angle x-ray (WAXS) diffraction was measured.
Silicalite was prepared both starting with a hydrogel and with a clear solution. In both cases crystallization nuclei were formed by transformation of (soluble) gels according to a hydrogel transformation mechanism.

## I. INTRODUCTION.

Usually zeolites are prepared starting from an amorphous gel, formed by a mixture of the appropriate chemicals. During a so-called induction or aging period transformations are taking place, followed by the formation of zeolites by crystallization from this amorphous phase.

On the mechanism of the transformations and the formation of crystals two general proposals have been formulated. According to the first, the amorphous gel phase reorganizes until a certain gel state has been developed, nucleation being followed by crystallization in this gel without participation of the liquid phase (hydrogel transformation mechanism). According to the second approach, the amorphous gel is partially dissolved by mineralizing agents during the pre-nucleation stage. From the species present in solution, nuclei will form and initiate the crystal growth, possibly influenced by a templating or cation-directing agent (solution mediated transport mechanism).

Detailed knowledge concerning these processes preceding nucleation of crystals in the reaction is difficult to obtain. Although methods such as adsorption techniques (BET) or transmission and scanning electron microscopy have been very informative concerning the porous structure of the zeolite crystals, applying these techniques to the amorphous gel state is often not appropiate. The physical and chemical structure of the amorphous gel phase obtained in the induction period changes during drying often resulting in irreversible damage to the vulnerable gel structures [1]. To study transformations in wet gels in situ non-invasive techniques are to be prefered, for example NMR [1,2]. However, because aggregates, particles and the corresponding gel transformations in zeolite precursors are on colloidal scale and information obtained by NMR is on molecular or sub-nanometer scale, an additional method is necessary to cover the 1 - 100 nm range.

Recently the application of small angle techniques has led to considerable advances in the determination of the structure and mechanisms of formation of oxide gels [3]. In this method the concept of fractality and fractal dimension [4] is very useful in applications and interpretations of small angle data in terms of aggregate morphology [5]. Although the relatively high concentrations in zeolite precursor gels prevent the formation of extended aggregates [6], using small angle neutron scattering (SANS) we showed both for silicalite [7] and zeolite A [8] concentration and temperature dependent transformations of the precursor gels preceding crystallization. Especially the in situ preparations of silicalite [7], using a special cell with zirconium windows allowing temperatures up to 190 °C, were very informative concerning the temperature dependent growth of precursor particles preceding and

during crystallization. Similar results were obtained for zeolite Na-Y with small angle x-ray scattering (SAXS) [9]. After aging at 50 °C the continuation at 100 °C was characterized by a transition from rough to smooth particles and during crystallization roughness increased again.

Because small angle scattering does not distinguish between amorphous and crystalline particles (the scale of the zeolitic porous structure is too small to be observed by SANS or SAXS), nucleation and growth of crystals can only be deduced by very careful matching of small angle diffraction data with wide angle x-ray diffraction data obtained in parallel experiments. With the often high sensitivity for temperature changes of the zeolite reaction mixtures results are sometimes not reliable and therefore a special experimental setup was constructed at Daresbury Laboratory (Warrington, UK) to measure simultaneously both small angle x-ray (SAXS) and XRD or wide angle x-ray scattering (WAXS) [10]. This SAXS-WAXS combination was used to investigate the amorphous and crystalline phases during the in situ preparation of silicalite. Also for this method a special constructed cell chamber had to be build to allow temperatures up to 195 °C [11].

Transformations observed in these studies suggest rather strongly that after a reorganization of the gel, nucleation and crystallization may occur within this gel without participation of the liquid phase (hydrogel transformation mechanism). To confirm this assumption also the preparation of silicalite from the solution phase was studied. In this experiment only soluble precursors were present and crystalline silicalite was precipitated from the clear solution.

**Fractal approach of scattering.**

In many objects the mass distribution can not be described correctly using Euclidean geometry. See figure 1 for an example.

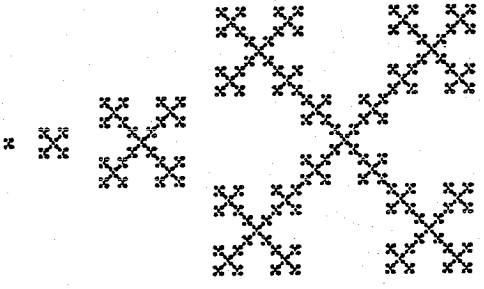

**Figure 1** Deterministic Vicsek fractal constructed of 1, 5, 25 and 125 basic units respectively. Fractal dimension D = 1.465.

In this figure the twodimensional pattern is build by repeated addition of the existing figure at the very end of the four branches. When the mass of the consecutive figures is calculated (the basic dots having mass m=1 and size d=1) the following relation between size R (= number of dots in a row) and mass M exists: if $R = 3^n$ then $M = 5^n$ with n = 1, 2, 3, 4 for the consecutive figures. Eliminating n gives the relation:

$$M = R^{\log 5/\log 3} \approx R^{1.465}$$

This is an unexpected result in terms of Euclidean geometry because in a twodimensional system the mass M is always related with a representative lengthscale R by expressions like $M = c.R^2$ with the constant c depending on the geometry of the figure. Due to the non-integer ("fractal") power in the mass-size relation of figure 1, the successive figures are called (deterministic) fractals.

In nature this kind of deterministic fractals are not observed. However, as can be shown [4,12], aggregates formed by diffusion or reaction limited cluster-cluster aggregation obey fractal laws: $M \propto R^D$ with exponent D the fractal dimension. In figure 2 an example, computer simulated and for clearness two-dimensional, is shown. Corresponding fractal aggregates in three dimensional space have D-values between 1 and 3.

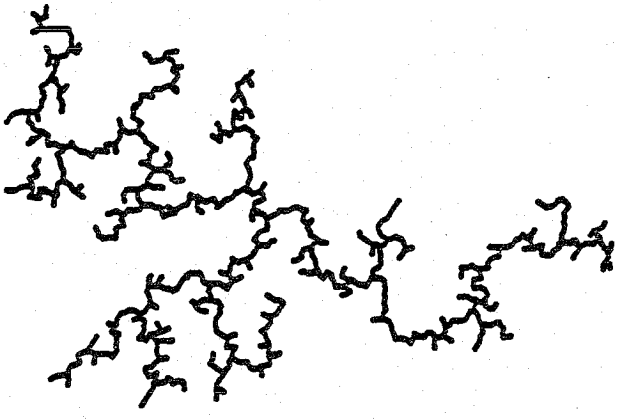

**Figure 2.** Two dimensional computer simulated aggregate (diffusion limited cluster-cluster aggregation).

These types of aggregates are also observed in silica gels prepared from water glass [5,13] and in many gels prepared according to principles of sol-gel chemistry [3,14].

Because x-rays are scattered mainly by inner shell electrons of the atoms, it is possible to obtain experimental information about density or density gradients in a system using scattered x-rays (neutrons scattered by nuclei of atoms give equivalent information). Because constructive and destructive interference of scattered radiation is controlled by Bragg's law, to observe with SAXS or SANS particles or structures in the range of 1 - 100 nm it is necessary to measure the the scattering pattern at very small angles ( $\Theta < 2°$) when radiation with wavelengths of approximately 0.1 nm is available. Introducing the scattering vector $Q = 2\pi/\lambda.\sin(2\Theta)$, particles with diameter d may be observed approximately at $Q = 2\pi/d$ $nm^{-1}$.

Low angle scattering at fractal systems can be represented schematically by figure 3. In this figure three Q-ranges may be discerned.

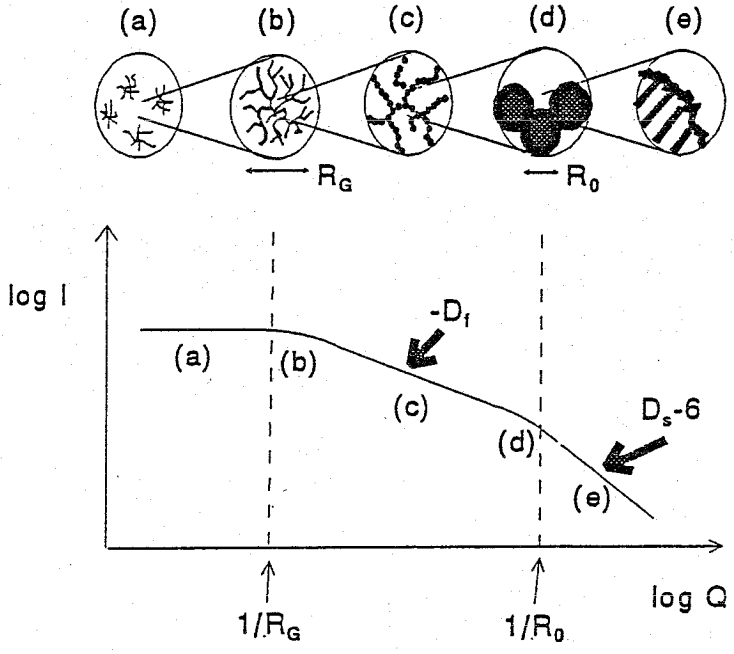


**Figure 3.** Log-log plot of small angle scattering spectra representing at increasing Q: collection of aggregates, an aggregate, part of an aggregate, primary particle and the (rough) surface of a primary particle.

a. $Q < \pi/R_g$ ($R_g$ = radius of gyration, in many cases $R_g \approx d/2$).
At these low angles radiation is scattered by relatively large-scale non-fractal objects. In silica gels [5,13] this might be a collection of many fractal aggregates, connected at the common peripheries and forming a continuous network: the gel. Although the individual aggregates are fractal, on very large scales the gel is a homogeneous network of local higher (aggregates) and local lower (space between the connected aggregates) density, resulting in a continuous non-fractal system.

b. $\pi/R_g < Q < \pi/R_o$ ($R_o$ = radius of elementary particles, the building blocks of the aggregates).
Because $R_g$ and $R_o$ are the obvious upper and lower limits of fractal aggregates, in this region the scattering due to the fractal aggregates is observed. Because the angle dependent intensity I(Q) will obey for fractals a power law relation given by $I(Q) = Q^{-D}$ [15], in the log(I)-log(Q) plot of figure 3 this region is characterized by a straight line with slope -D. Therefore fractal objects can be recognized inmediately from scattering spectra (provided the fractal range is a decade or more) and fractal dimensions can be extracted directly from these spectra.

The upper and lower limits of the fractal region are also very informative. The cross-over to the non-linear low Q region at $\pi/R_g$ gives approximately the radius of the fractal aggregate and from the crossover at high Q the radius of the elementary particles can be determined.

c. $Q > \pi/R_o$ (Porod region).
When the elementary particles are smooth spheres, the slope in the Porod region in a log(I)-log(Q) plot will be a straight line with slope = -4 [16].

However, if the surface is not smooth but can be described by a surface fractal with surface fractal dimension $D_s$, then $I(Q) \sim Q^{-(6-Ds)}$ [17,15] and the slope of the Porod region in the log(I)-log(Q) plot will be $D_s$-6 instead of -4. The fractal dimension $D_s$ of a fractal surface will always be between 2 (smooth surface) and 3 (extremely rough surface; the "surface" is transformed into a very porous 3-dimensional system).

## II. EXPERIMENTAL SECTION.

### Small and wide angle X-ray scattering

The combined small and wide angle X-ray scattering experiments were performed using beamline NCD 8.2 at the synchrotron radiation source at the Daresbury Laboratories, United Kingdom. See figure 4 for a schematic representation of the experimental SAXS-WAXS set up.

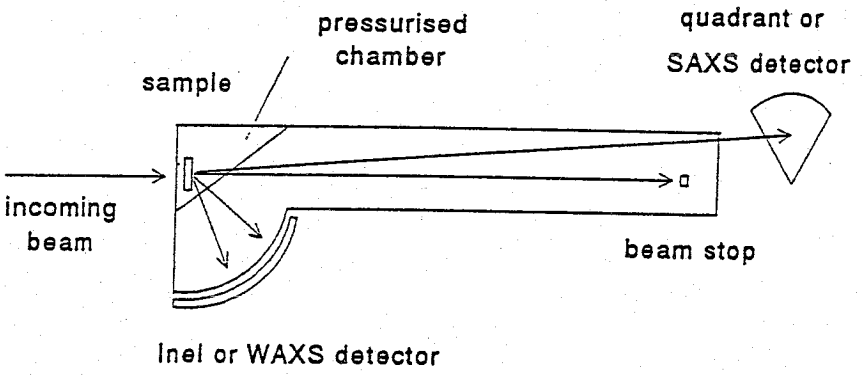


**Figure 4.** Schematic representation of the experimental SAXS-WAXS set up.

The length of the vacuum chamber is 3.5 m. Details concerning camera geometry and data collection were presented extensively elsewhere [10].

The spatial resolution of the SAXS quadrant detector is 400 $\mu$m and it can handle up to 300000 coumts $s^{-1}$. The WAXS detector is a curved knife-edge INEL detector with a spatial resolution of 50 $\mu$m and can handle up to 100000 counts $s^{-1}$. The Q-ranges covered with both detectors are $0.01 < Q < .175$ Å$^{-1}$ and $0.8 < Q < 3.4$ Å$^{-1}$ for the SAXS and WAXS detector respectively. The wavelength of the X-rays is 0.15 nm and $\Delta\lambda/\lambda < 4.10^{-3}$. The SAXS data were corrected for background scattering and solvent using the procedure introduced by Vonk [18]. The Q-axis of the SAXS pattern was calibrated with an oriented specimen of wet rat tail collagen. A fully crystallized specimen of zeolite A (NaA, Proctor and Gamble) was used to calibrate the Q-axis of the WAXS pattern. Fractal dimensions were determined from the parts of the

scattering curves where power-law behaviour was observed and particle or aggregate sizes were determined from the point of deviation from this power-law behaviour. The scattering slope $\alpha$ is related to the mass fractal dimension as - $\alpha$ = D and to the surface fractal dimension as $\alpha$ = ($D_s$ - 6) (figure 3).

When performing hydrothermal experiments at elevated temperatures care has to be taken that no water is lost from the sample due to cell leakage. Therefore a sealed sample chamber was constructed which could be both temperature and pressure controlled. The actual brass reaction cell was placed in this chamber and was temperature controlled with the help of a resistance heater and a PID controller. The sample chamber was pressurised with dry nitrogen to the vapour pressure of water at the relevant temperature. In this way the mica windows of the sealed reaction cell are subjected to a small pressure differential and consequently the water does not evaporate from the sample. The pressurised chamber and reaction cell were constructed such that the X-ray path length was minimised in order to reduce absorption and background scatter. The sample chamber was separated from the camera vacuum by a 125 micron Kapton window.

## Materials

The heterogeneous reaction mixture was prepared using Aerosil 380 (Degussa AG) as a silica source. Sodium hydroxide (Merck p.a.) and the template tetrapropylammonium bromide (Aldrich-Chemie 98%) were dissolved in demineralized water. Then the silica was added and stirred until a smooth smurry was obtained. Finally the remaining water was dosed and the stirring was continued until the reaction mixture had a uniform consistency. The following molar ratio's were used: $SiO_2$/TPA = 6.25, $SiO_2$/NaOH=12.8 and $H_2O$/$SiO_2$=13.8 [19]. The reaction temperature was 190 °C.

The homogeneous synthesis silicalite reaction mixture [20] was prepared from silicic acid powder (Baker, 10,2 wt% water), NaOH pellets (Merck, >99wt%) and tetrapropyl ammonium (Fluka 20 wt%) in the following molar ratios: $SiO_2$/TPA=4.1, $SiO_2$/NaOH=11.5, $H_2O$/$SiO_2$=11. NaOH was added to the TPAOH solution with gentle mixing. Then the silicic acid was added to the solution and stirred until a homogeneous dispersion was obtained. This solution was then heated for approximately 10 minutes to obtain a clear synthesis precursor mixture and was corrected for water loss during heating. This synthesis mixture remains usually clear during reaction until crystallization, detectable with standard X-ray diffraction [20], occurs. The reaction temperature was 120 °C ± 5 °C.

## III. RESULTS & DISCUSSION.

### Heterogeneous silicalite nucleation.

In figure 5 the SAXS spectra (a), (b) and a three-dimensional plot of the WAXS spectra (figure 6) of the heterogeneous synthesis of silicalite are shown as a function of time. For clearity reasons not all SAXS spectra have been shown. The slopes $\alpha$, calculated with a least-squares fit from the log-log plots from the SAXS spectra in the range -0.7 < log Q < -1.6 $Å^{-1}$, are ranging between -3.4 and -4.0. Refering to the discussion of figure 3, it is obvious that the amorphous precursor system exhibits surface-fractal behaviour ($2 < D_s < 2.6$). The power-law behaviour of the scattering extends over approximately one decade. Contrary to the SANS experiments [7] on the same synthesis gels no radius of gyration of amorphous zeolite particles could be derived from the SAXS spectra because the accessible low Q-range is not the same in the SANS and SAXS experiments. The value found for the starting reaction mixture, $D_s = 6 + \alpha = 2.7$, is within the experimental error, equal to the value previously found with SANS (2.6). This value is indicative for a very rough surface structure.

The same SANS experiments [7] as mentioned earlier performed at elevated temperatures showed a displacement of the scattering pattern to smaller Q-values and a decrease of the surface fractal dimension from 2.7 to 2.25 (at 130, 150, 170 and 190 °C) The radius of gyration or particle size of the unreacted precursor mixture was approximately 14 nm and increased as a function of reaction time. At higher temperatures (170, 190 °C) these particles grow rapidly but at lower temperatures larger sizes are obtained. Particles grow and are smoothed by addition of amorphous material from the amorphous bulk. Growth is observed both before as well as after crystallization indicating that the crystallization starts in or on the growing gel particles.

The decrease of the surface fractal dimension is also observed in the SAXS pattern obtained at 190 °C. The values of the surface fractal dimension as found with SAXS are smaller than the values found in the SANS experiment. No significant displacement in the SAXS spectra as a function of time was observed (figure 5). After approximately 50 minutes reaction no changes in surface roughness are observed while the amount of crystallinity is increasing. This implies that the electron scattering density of the reorganised, amorphous particles is equal to the electron density of the zeolite crystals.

The WAXS spectrum shown in figure 6 indicate no signs of crystallinity after short reaction times. The bump observed at

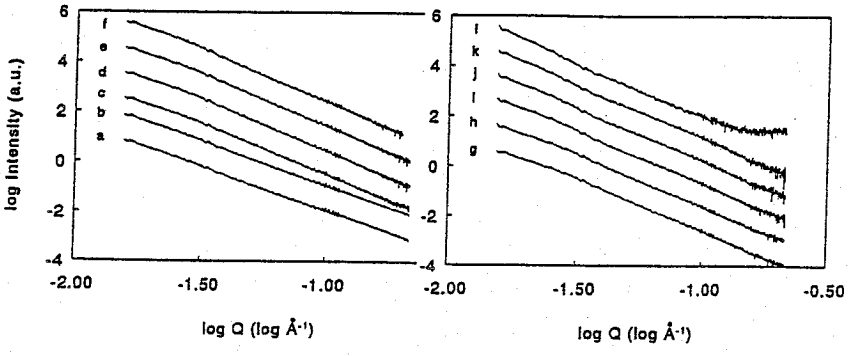


**Figure 5.** Small angle x-ray scattering spectra during silicalite synthesis performed at 190 °C after: (a) 0 min., (b) 10 min., (c) 20 min., (d) 32 min., (e) 41 min., (f) 48 min., (f) 48 min., (g) 54 min,. (h) 61 min., (i) 106 min., (j) 156 min., (k) 206 min., (l) 256 min. The spectra have been shifted vertically for clarification and intensity is expressed in arbitrary units.

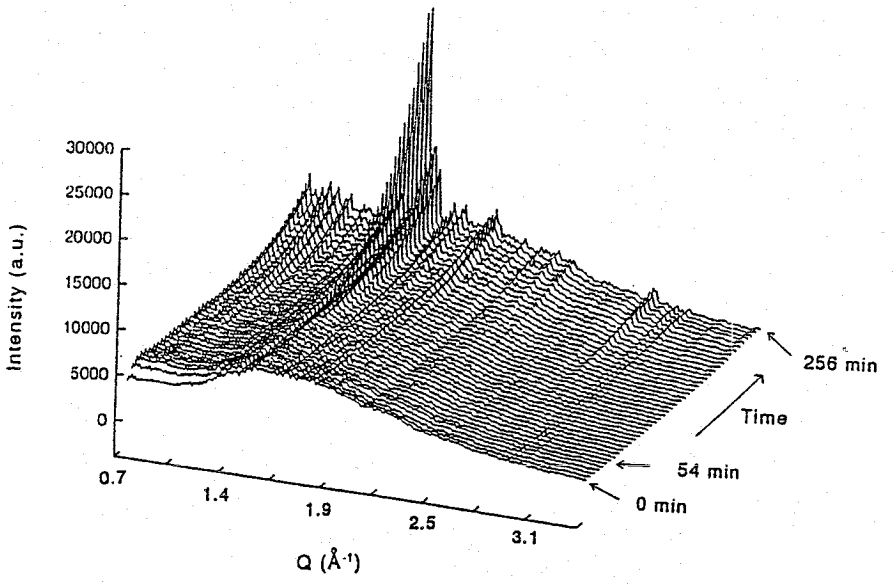


**Figure 6.** Intensity (arbitrary units) of WAXS spectra as a function of time during silicalite synthesis performed at 190 °C.

approximately Q = 1.6 $Å^{-1}$ (2Θ = 26°) is due to amorphous scattering from water present in the reaction mixture. Crystallization of silicalite starts after 54 minutes of reaction as can be observed in the WAXS spectra (figure 6) where a peak at 2Θ = 23.2° starts to grow. This is known to be the most intense peak in the diffraction pattern of silicalite [21]. Unfortunately two other very intense peaks in the XRD-pattern of silicalite (2Θ = 7.9 and 8.9) can not be observed due to the small data gap between the SAXS and WAXS detectors. The peaks grow gradually and after 256 minutes the maximum crystallinity is reached. After prolonged reaction times the intensity of the diffraction peaks and the SAXS signal decreased due to sedimentation of the zeolite crystals in the reaction cell.

In figure 7 the diffraction spectra of the final product, measured both with WAXS and with a standard diffraction apparatus (XRD) are compared. The peaks of the XRD spectrum are better resolved due to limited number of data points (maximum 512) available on the Inel-WAXS detector. The WAXS spectrum was recorded in 5 minutes while the XRD spectrum was obtained in 30 minutes over the same angular range. The signal to noise ratio in the WAXS spectra is sufficient after 1 minute of data collection, but the accumulation time was set to 5 minutes to obtain an adequate signal to noise ratio for the SAXS spectrum.

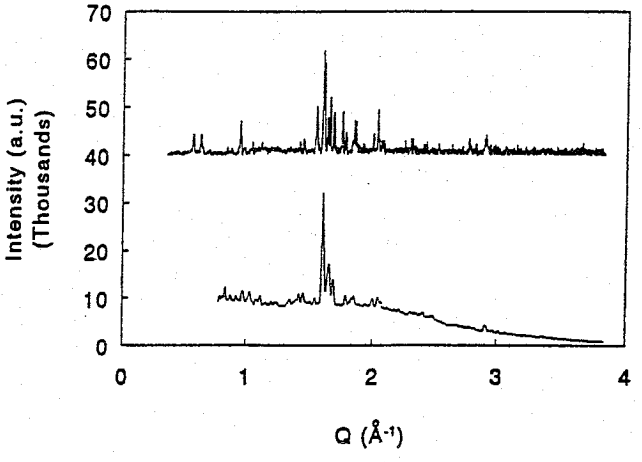


**Figure 7.** Diffraction spectra of the final state of the silicalite synthesis performed with the SAXS-WAXS set up. The top curve isthe diffraction spectrum produced with the standard XRD apparatus. The bottom curve the diffraction spectrum produced with the SAXS-WAXS equipment.

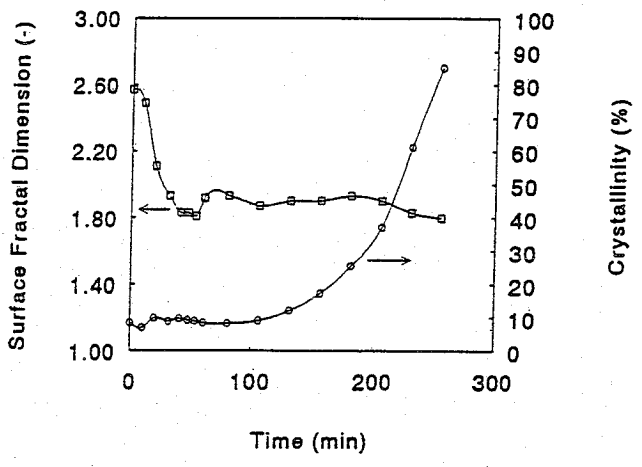


**Figure 8.** Development of the surface fractal dimension and crystallinity during the synthesis of silicalite at 190 °C.

In figure 8 the progress of crystallinity is plotted together with the progress of the surface fractal dimension as a function of time. The crystallinity from the WAXS spectrum was normalised with the help of the XRD spectrum and was found to be approximately 85% for the final product.

It can be seen that the crystallization starts after the surface roughness of the particles has become constant as a function of time (surface fractal dimension constant, see figure 8). This implies the need for a reorganisation of the amorphous gel phase before crystallization can take place or a reorganisation in the precursor phase during which crystallization nuclei are formed. In the latter case, however, these nuclei are too small to be observed by WAXS.

It appears that also in the homogeneous system cluster aggregation occurs before crystallization. SAXS curves measured for homogeneous silicalite synthesis and corresponding aggregate structures (schematic) are shown in figure 9 and figure 10 respectively. As figure 9a and 10b show, the aggregate morphology (D = 2.2), observed after 5 minutes reaction, is typical for aggregates, formed according to reaction limited cluster-cluster aggregation [4]. The low rate of reaction is due to the effect of the structure directing TPA ions [22].

The size, $d=2 \bullet R_g$ (=2•radius of gyration) of the reaction limited aggregate formed is approximately 6.4 nm. These aggregates are built from primary particles with a radius smaller than 1.6 nm, the upper Q-

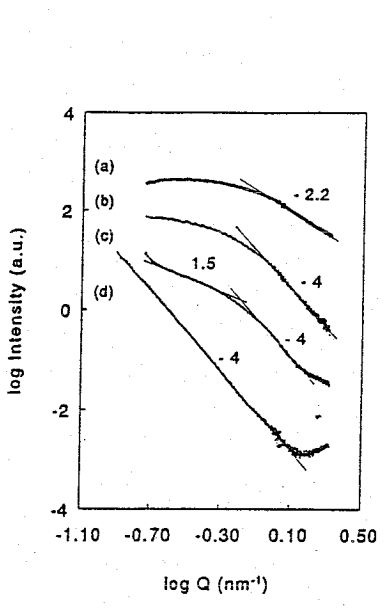


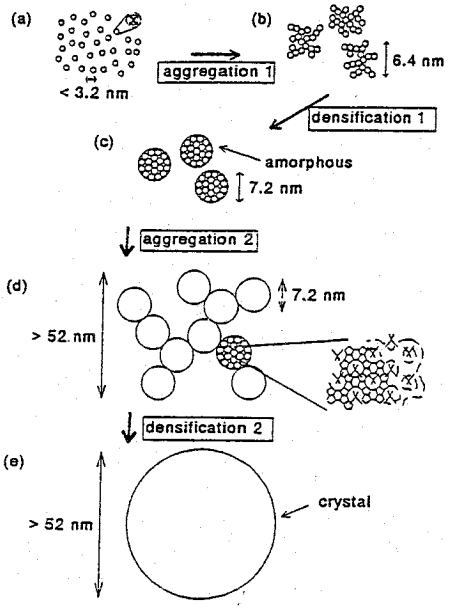


**Figure 9.** (left) Small angle x-ray scattering spectra of the clear silicalite reaction mixture after various reaction times: (a) 5 min., (b) 35 min., (c) 75 min. and (d) 105 min.

**Figure 10.** (right) Mechanism of micro-structural random packing, subsequent ordering and crystallization. (a) shows the silicate/TPA clusters in solution, (b) primary fractal aggregates formed from the silicate/TPA clusters (6.4 nm, SAXS in figure 9a), (c) densification of these primary fractal aggregates (SAXS figure 9b), (d) combination of the densified aggregates into a secondary fractal structure and crystallization (SAXS in figure 9c) and (e) densification of the secondary aggregates and crystal growth (SAXS in figure 9d).

limit of the available SAXS range. These primary particles may be hydrated tetrapropylammonium-silicate clusters. Burkett and Davis [2] have provided evidence for the existence of pre-organised organic-inorganic composite structures in the synthesis of ZSM-5. Short range intermolecular interactions exist between the protons of TPA and silicon atoms of the zeolite precursor phase before development of the long range order indicative of the ZSM-5 structure [2].

The observed clusters start to densify (figure 9b & 10c) as a function of time into denser mass fractal aggregates and subsequently into surface fractal aggregates until after 35 minutes reaction at 120°C a Porod slope (slope = - 4) is observed indicative for a homogeneous dense structure with a smooth surface. The size of this structure is only very slightly increasing (to 7.2 nm) with time c.q. not decreasing upon densification, indicative for the transport of additional primary particles (TPA/silicate cluster) or silica particles from solution to the cluster. The size of these secondary particles is approximately equal to 20 silicalite unit cells.

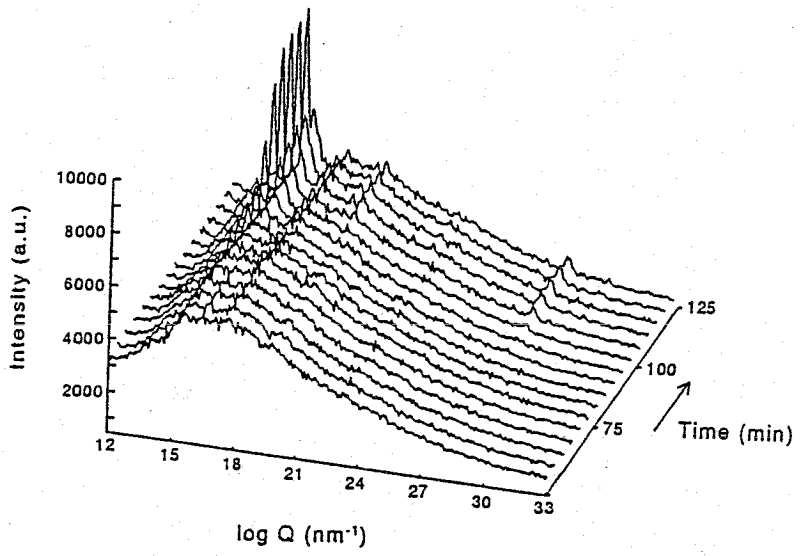


**Figure 11.** WAXS spectra of clear silicalite synthesis mixtures to demonstrate crystallization between 50 and 125 minutes of reaction.

After this densification, the 7.2 nm clusters aggregate again into a new fractal aggregate (figure 9c & 10d). At the same moment crystallinity is observed with WAXS. In figure 11 the WAXS curves are plotted and in figure 12 a survey curve is shown with the scattering slope at large Q (small particles), at small Q (large particles or clusters) and the percentage crystallinity as determined with WAXS. From this we may conclude that crystallization starts as soon as the dense clusters of 7.2 nm have been formed and aggregation into the larger aggregate starts. Growth of zeolite particles occurs by transformation of the aggregated clusters that form the new fractal structure (figure 9c). Crystallization occurs again via surface fractal aggregates to a completely smooth

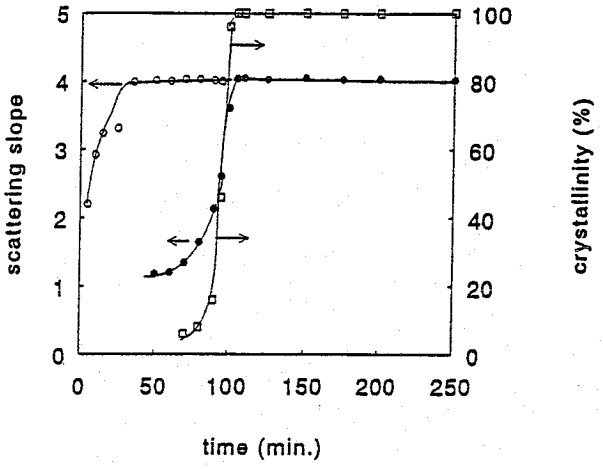


**Figure 12:** Combination curve of crystallinity (from WAXS) and micro-structure (from SAXS). The scattering slopes obtained with SAXS are divided in the scattering slope at (o) high Q (small r) and the scattering slope at (•) small Q (large r) to clearly demonstrate the consistence between the micro-structure and crystallization (□).

structure (figure 9d & 10e). They grow rapidly to a size larger than the upper size limit (low Q-limit) of the available SAXS range (d > 52 nm).

Crystal growth occurs by combination of the densified primary aggregates into the secondary aggregates, indicative for growth by combination of already growing nuclei. These results are in agreement with the results obtained by Twomey et al. [23] who deduced from size distributions of crystals obtained from light scattering experiments that nucleation is a continuous process and that further growth of nuclei occurs by agglomeration of nuclei that are already growing.

One interesting feature of the results presented is that also in the homogeneous system a precursor aggregate is formed before crystallization, indicative for a gel transformation or gel reorganisation mechanism of zeolite crystallization even in a clear silicalite solution. This is in contrast to the direct homogeneous crystallization.

For the heterogeneous silicalite synthesis performed with much higher silica concentrations it was concluded that crystallisation proceeded also according to a gel transformation mechanism. No mass fractality was observed during these experiments. The very high silica concentration leads to very compact amorphous surface fractal precursor particles with an initial particle size of 28 nm. Crystallization however, starts only after

the surface fractal amorphous particles have been transformed to smooth particles with $D_s=2$. An analogous feature was observed in this study. The mass fractal aggregate had to transform into smooth, homogeneous dense structures before crystallization starts. From this we may conclude that homogeneous and heterogeneous crystallization both need an intermediate gel phase before nucleation and crystallization can occur.

In the gel phase nucleation and crystallization occurs more slowly than in the homogeneous phase, because the gel formed will first have to dissolve before a new phase is formed from which crystallization can occur. This dissolution step is not required in the homogeneous phase, where the mass transport and subsequent formation of the primary and secondary clusters seems to be the rate determining step. Instant crystallization may be achieved when preparing the precursors in such a way that directly the desired gel phase for nucleation is obtained.

**Acknowledgements.**

Financial support was provided by the Dutch Department of Economic Affairs, as part of the IOP-Catalysis program. We are indebted to dr. W. Bras for his help and assistance in performing the SAXS-WAXS measurements at station 8.2, Daresbury Laboratory. Support and access to Daresbury Laboratory under the terms of the HCMP-program of the European Community is also gratefully acknowledged.

**References.**

1. D.M. Ginter, G.T. Went, A.T. Bell en C.J. Radke, Zeolites, 12 (1992) 733 and 743.
2. S.L. Burkett and M.E. Davis, J.Phys.Chem., 98 (1994) 4647.
3. J.D.F. Ramsay, Chem.Soc.Rev., 15 (1986) 335.
4. R. Jullien and R. Botet, Aggregation and Fractal Aggregates, World Scientific, Singapore, 1986
5. T.P.M. Beelen, W.H. Dokter, H.F. van Garderen and R.A. van Santen, Adv.Coll.Interfac.Sci., 50 (1994) 23.
6. H.F. van Garderen, E.Pantos, W.H. Dokter, T.P.M. Beelen and R.A. van Santen, Modelling Simul. Mater. Sci. Eng., 2 (1994) 295.
7. W.H. Dokter, T.P.M. Beelen, H.F. van Garderen, C.P.J. Rummens, R.A. van Santen and J.D.F. Ramsay, Coll.& Surf. A., 85 (1994) 89.
8. T.P.M. Beelen and W.H. Dokter, ISIS Annual Report, vol II, 1994,

369
9. T.P.M. Beelen, W.H. Dokter, H.F. van Garderen, R.A. van Santen and E. Pantos, J.Phys.IV (France), Coll. C8, 3 (1993) 393.
10. W. Bras, G.E. Derbyshire, A.J. Ryan, G.R. Mant, A. Felton, R.A. Lewis, C.J. Hall and G.N. Greaves, Nucl.Instrum.Meth.Phys.Res., A326 (1993) 587.
11. W.H. Dokter, T.P.M. Beelen, H.F. van Garderen, R.A. van Santen, W. Bras, G.E. Derbyshire and G.F. Mant, J. Appl.Cryst., 27 (1994) 901
12. P. Meakin, in H.E. Stanley and N. Ostrowski (Eds), On growth and form, NATO ASI Ser. E100, Martinus Nijhof, Dordrecht, 1986.
13. a) P.W.J.G. Wijnen, T.P.M. Beelen, C.P.J. Rummens, H.C.P.L. Saeijs and R.A. van Santen, J. Appl. Cryst., **24** (1991) 759.
b) P.W.J.G. Wijnen, T.P.M. Beelen, C.P.J. Rummens and R.A. van Santen, J. Non-Cryst. Sol., **136** (1991) 119.
14. C.J. Brinker and G.W. Scherer, Sol-gel science:the physics and chemistry of sol-gel processing, Academic Press, London, 1990.
15. J.E. Martin and A.J. Hurd, J.Appl.Cryst. 20 (1987) 61.
16. O. Glatter and O. Kratky (Eds), Small Angle X-Ray Scattering, Academic Press, New York, 1982.
17. H.D. Bale and P. Schmidt, Phys.Rev.Lett., 53 (1983) 596.
18. C.G. Vonk, J.Appl.Cryst., 6 (1973) 81.
19. J. El Hage-Al Asswad, N. Dewaele, J.B. Nagy, R.A. Hubert, Z. Gabelica, E.G. Derouane, F. Crea, R. Aiello and A. Nastro, Zeolites, 8 (1988) 221.
20. J.P. Verduijn, PCT/EP92/02386.
21. R. von Ballmoos, Collection of simulated xrd powder patterns for zeolites, Butterworth Scientific Limited, Guildford.
22. E.M. Flanigen, in H. van Bekkum, E.M. Flanigen and J.C. Jansen (Eds.), Introduction to zeolite science and practice, Elsevier Science Publishers B.V. , Amsterdam, 1991
23. T.A.M. Twomey, M. Mackay. H.P.C.E. Kuipers and R.W. Thompson, Zeolites, 14 (1994) 162